Reactivation of the p53 pathway as a treatment modality for KSHV-induced lymphomas

Grzegorz Sarek,[1] Sari Kurki,[2,3] Juulia Enbäck,[2] Guergana Iotzova,[4] Juergen Haas,[4] Pirjo Laakkonen,[2] Marikki Laiho,[2,3] and Päivi M. Ojala[1]

[1]Genome-Scale Biology Program, Biomedicum Helsinki, Institute of Biomedicine, [2]Molecular and Cancer Biology Program, Biomedicum Helsinki, Institute of Biomedicine, and [3]Haartman Institute, University of Helsinki, Helsinki, Finland. [4]Max von Pettenkofer Institut LMU-München, Munich, Germany and School of Biomedical Sciences, College of Medicine, University of Edinburgh, Edinburgh, United Kingdom.

Kaposi's sarcoma herpesvirus (KSHV) is the etiologic agent for primary effusion lymphoma (PEL), a non–Hodgkin type lymphoma manifesting as an effusion malignancy in the affected individual. Although KSHV has been recognized as a tumor virus for over a decade, the pathways for its tumorigenic conversion are incompletely understood, which has greatly hampered the development of efficient therapies for KSHV-induced malignancies like PEL and Kaposi's sarcoma. There are no current therapies effective against the aggressive, KSHV-induced PEL. Here we demonstrate that activation of the p53 pathway using murine double minute 2 (MDM2) inhibitor Nutlin-3a conveyed specific and highly potent activation of PEL cell killing. Our results demonstrated that the KSHV latency-associated nuclear antigen (LANA) bound to both p53 and MDM2 and that the MDM2 inhibitor Nutlin-3a disrupted the p53-MDM2-LANA complex and selectively induced massive apoptosis in PEL cells. Together with our results indicating that KSHV-infection activated DNA damage signaling, these findings contribute to the specificity of the cytotoxic effects of Nutlin-3a in KSHV-infected cells. Moreover, we showed that Nutlin-3a had striking antitumor activity in vivo in a mouse xenograft model. Our results therefore present new options for exploiting reactivation of p53 as what we believe to be a novel and highly selective treatment modality for this virally induced lymphoma.

Introduction

Kaposi's sarcoma herpesvirus (KSHV) is a DNA tumor virus and causative agent in 3 different tumor types: Kaposi's sarcoma (KS), a plasmablastic variant of multicentric Castelman's disease (MCD), and an AIDS-related form of B cell lymphoproliferative disorder called primary effusion lymphoma (PEL) (1–3). Additionally, KSHV infection is suggested to be linked to other types of lymphoproliferations (reviewed in ref. 4). PEL is a non–Hodgkin type lymphoma latently infected with KSHV and manifests as an effusion malignancy in KS patients with advanced AIDS, but it may also occur in HIV-negative individuals (reviewed in refs. 5, 6). The KSHV genome encodes several homologs of cellular proteins, which engage cellular signaling pathways, govern cell proliferation, and modulate apoptosis (reviewed in ref. 7). Latent viral genes include a cluster of 3 genes transcribed from the same promoter, encoding *latency-associated nuclear antigen* (*LANA*), *viral cyclin*, and *viral FLICE-inhibitory protein*. Similar to oncogenic proteins of other tumor viruses, these proteins are known to regulate the major tumor suppressor pathways (cell cycle, apoptosis, and cell survival), suggesting a role for them in oncogenesis of this lymphoma.

p53 is a transcription factor that plays a central role in protecting cells from tumor development by inducing cell-cycle arrest or apoptosis via a complex signal transduction network referred to as the p53 pathway (reviewed in ref. 8, 9). The *p53* gene is mutated or deleted in 50% of all malignant tumors (reviewed in ref. 10). The other half of human cancers express WT p53 protein, which upon reactivation is capable of inducing apoptosis in cancer cells, thus offering a potential therapeutic opportunity applicable to a wide range of human tumors. Because tumor cells are prone to p53-induced apoptosis as a result of oncogene activation, it is possible that p53-based anticancer strategies may not require selective targeting of tumor cells (11–13). A recently discovered strategy for p53 activation targets the interaction of p53 with its negative regulator, murine double minute 2 (MDM2), an E3 ubiquitin ligase that binds p53 and facilitates its ubiquitin-dependent degradation (14). Vassilev et al. (15) have developed potent and selective small-molecule inhibitors of p53-MDM2 interaction, the nutlins, which activate the p53 pathway in vitro in cells with WT p53 and cause cell-cycle arrest via induction of $p21^{CIP1}$ and, in some case, apoptosis. Although mechanisms converting the Nutlin-3a–induced cytostatic pathways to cytotoxic pathways are not fully understood, the fact that Nutlin-3a has showed potent antitumor activity in certain mouse xenograft models suggests that it is a potential treatment option for cancers with WT p53 (15, 16).

PELs are aggressive KSHV-induced lymphomas, with median survival times reported to be shorter than 6 months after diagnosis (17). Despite some interesting new therapeutic leads such as inhibition of NF-κB signaling (18, 19) or RNA interference against viral latent proteins (20), the current clinical treatments based on high-dose chemotherapy regimens are neither potent nor selective for this cancer (21, 22), and PEL remains a fatal disease. Although *p53* mutations are relatively common in hematopoietic malignancies, the majority of the PELs appear to have WT p53 (23–25), suggesting that genetic alterations in the *p53* gene are not selected for during PEL tumorigenesis. However, the pathogenetic mechanisms leading to lymphomas by this oncogenic

Nonstandard abbreviations used: ATM, ataxia telangiectasia mutated; 53BP1, p53 binding protein 1; Chk2, checkpoint kinase 2; KS, Kaposi's sarcoma; KSHV, Kaposi's sarcoma herpesvirus; LANA, latency-associated nuclear antigen; LCL, lymphoblastoid cell line; MDM2, murine double minute 2; PEL, primary effusion lymphoma; PI, propidium iodide; rKSHV, recombinant KSHV.

Conflict of interest: The authors have declared that no conflict of interest exists.

Citation for this article: *J. Clin. Invest.* **117**:1019–1028 (2007). doi:10.1172/JCI30945.

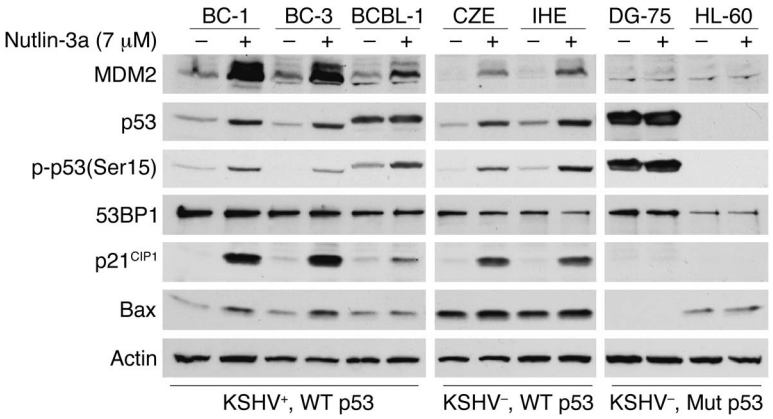

Figure 1
Nutlin-3a activates p53 and its target genes in PEL cells. KSHV-infected PEL cells (BC-1, BC-3, and BCBL-1), EBV-transformed LCLs (CZE and IHE), and cells with mutant p53 (DG-75 and HL-60) were incubated for 12 hours in the presence (+) or absence (–) of 7 μM Nutlin-3a. Whole-cell lysates were subjected to SDS-PAGE followed by Western blotting and analyzed for p53, MDM2, phosphorylated-p53(Ser15) [p-p53(Ser15)], 53BP1, $p21^{CIP1}$, and Bax expression. Actin immunoblot is shown as a loading control.

tumor virus are unknown. Two previous reports have suggested that upon exogenous expression, LANA interferes with p53 and inhibits its transcriptional activity (26, 27). More recently, LANA was also suggested to function as a component of the EC5S ubiquitin complex targeting p53 for degradation (28). However, these findings have not progressed toward a mechanistic explanation of how the virus overcomes normal cellular barriers or provided opportunities for therapy.

Here we studied p53 signaling and nongenotoxic activation of the p53 pathway in PEL cells. We demonstrate that a small-molecule inhibitor of the p53-MDM2 interaction, Nutlin-3a, efficiently activated the p53 pathway in several PEL cell lines expressing WT p53, leading to cell-cycle arrest and massive apoptosis. The cytotoxic effect of Nutlin-3a was specific for the KSHV-infected cells, as Nutlin-3a did not induce apoptosis in lymphoblastoid cell line (LCLs) transformed with EBV despite their expression of WT p53. We present data for the mechanisms underlying this specificity and demonstrated the antitumor activity of Nutlin-3a using a mouse xenograft model of PEL. Taken together, our results suggest that activation of the p53 pathway may be an effective treatment for KSHV-infected lymphomas.

Results

Nutlin-3a stabilizes p53 and activates the p53 pathway in PEL cells. Targeting the p53-MDM2 interaction by using small-molecule inhibitors is a promising strategy for anticancer therapy in tumor cells retaining WT p53. One of these compounds, Nutlin-3a, mimics a p53 peptide by competitively binding MDM2 at the p53 binding pocket, which activates the p53 pathway (15). To explore whether the p53 pathway is functional in PEL cells, we first examined the effect of Nutlin-3a on accumulation of p53 and induction of its target gene expression. Treatment of asynchronously growing PEL cell lines BC-1 and BC-3 with 7 μM Nutlin-3a for 12 hours resulted in a strong and specific increase (12- to 15-fold) in the expression levels of p53, MDM2, $p21^{CIP1}$, and Bax (Figure 1). In PEL cell line BCBL-1, the regulation of the p53 targets was attenuated (Figure 1). Interestingly, BCBL-1 cells have previously been shown to harbor a *TP53* missense mutation (M246I; ref. 25) in one copy of the *TP53* gene (29), providing a possible explanation for the attenuated response. Interestingly, PEL cells express relatively high levels of p53 binding protein 1 (53BP1), a component of the ataxia telangiectasia mutated–checkpoint kinase 2 (ATM-Chk2) DNA damage checkpoint pathway (30, 31) recently identified as a critical mediator of cellular cytotoxicity by Nutlin-3a (27). To address the specificity of Nutlin-3a treatment on KSHV lymphomas, we also treated EBV-transformed LCLs, which express WT p53. Exposure of EBV-transformed LCLs CZE and IHE to Nutlin-3a resulted in increased levels of p53, MDM2, and $p21^{CIP1}$. Both PEL cells and EBV-transformed LCLs also showed a specific increase in the expression of activated p53, detected using an antibody specific for p53 phosphorylated on serine 15 (Figure 1). However, the expression of Bax did not change notably in the EBV-transformed LCLs upon Nutlin-3a treatment (Figure 1). Treatment of EBV-negative Burkitt lymphoma cells constitutively expressing high levels of mutant p53 (cell line DG-75) or the p53-deficient cell line HL-60 did not result in activation of the p53 pathway (Figure 1). This confirmed that Nutlin-3a activated the p53 pathway only in cells with functional WT p53.

Nutlin-3a induces cell-cycle arrest in PEL cells. Induction of p53 activity halts the cell cycle through transcriptional upregulation of the cyclin-dependent kinase inhibitor $p21^{CIP1}$, which causes G_1-S and G_2-M cell-cycle arrest (32). To explore whether Nutlin-3a–induced p53 activation causes cell-cycle arrest, we performed flow cytometric analyses of PEL cells, EBV-transformed LCLs, and p53 mutant cells treated with the MDM2 inhibitor. Cells were exposed to Nutlin-3a for 12, 24, or 48 hours, labeled with BrdU, and analyzed by multiparameter flow cytometry. As expected, treatment of PEL cells with Nutlin-3a markedly increased the G_1/S ratio of the cells over that of untreated controls, reflecting an efficient G_1 arrest. We found that the proportion of S-phase cells was considerably decreased in BC-1 and BC-3 cells as soon as 12 hours after incubation. The S-phase fraction in BCBL-1 cells also decreased, but only after 24 hours, consistent with our results of delayed p53 upregulation in these cells. Incubation for 48 hours led to a complete depletion of the S-phase cells and their profound accumulation in the G_1 phase in all PEL cell lines studied (Figure 2A). Interestingly, we also observed that accumulation in the sub-G_1 phase was increased in Nutlin-3a–treated cells compared with untreated cells (Figure 2A, arrows). After 48 hours of treatment, the sub-G_1 population reached 41%, 36.4%, and 18.7% in BC-1, BC-3, and BCBL-1 cells, respectively, suggesting increased cell death. In the KSHV-negative EBV-transformed LCLs CZE and IHE, the treatment led to an efficient G_1-phase arrest, but there was no obvious increase in the sub-G_1 population (Figure 2B). Importantly, even an extended 96-hour exposure to Nutlin-3a was insufficient to markedly increase the sub-G_1 population in EBV-transformed LCLs (data not shown). Cell-cycle analysis of the mutant p53 cell lines DG-75 and HL-60 showed profiles indis-

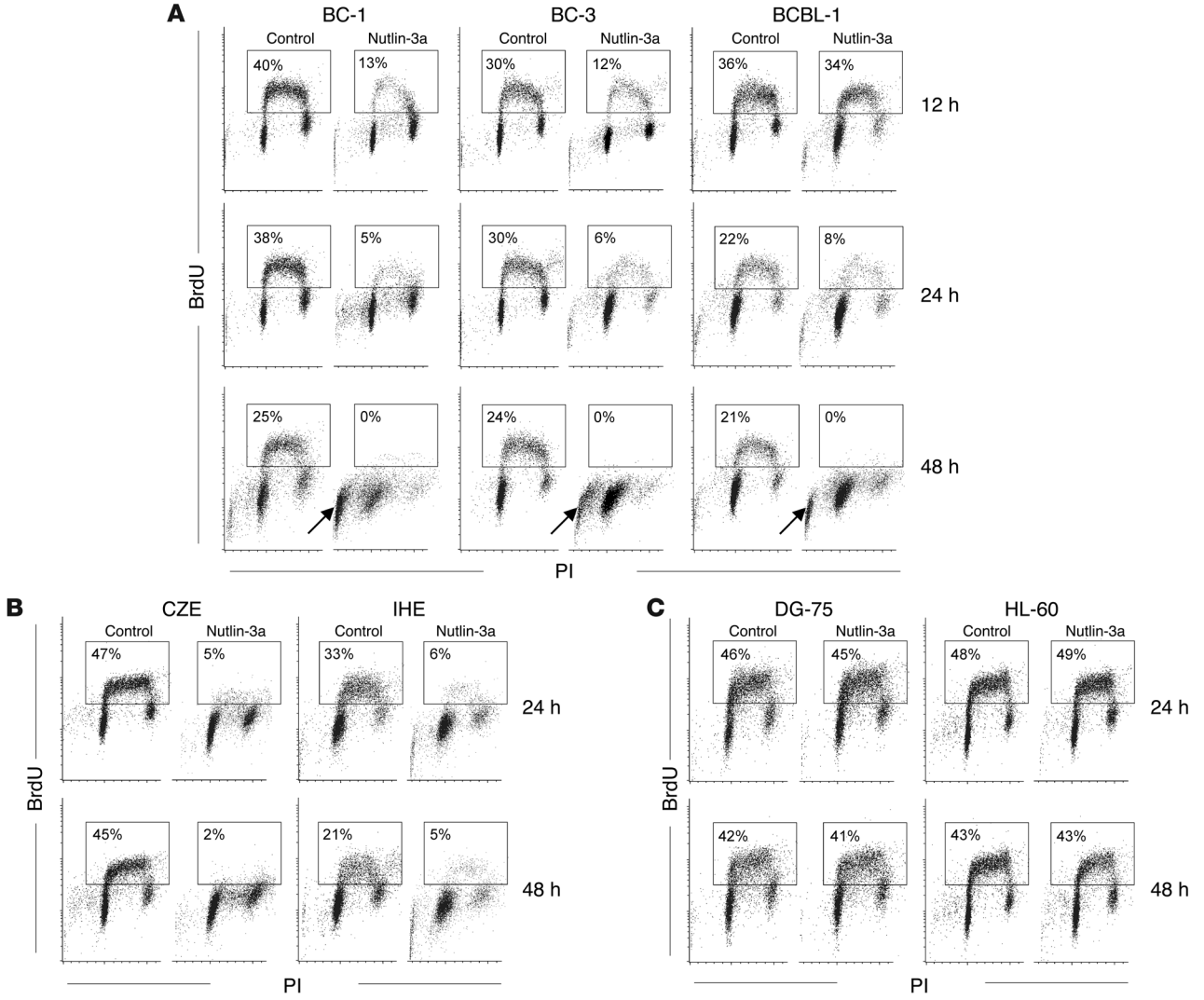

Figure 2

Nutlin-3a induces cell-cycle arrest in PEL cells and EBV-transformed LCLs. Asynchronously growing PEL cells (BC-1, BC-3, and BCBL-1; **A**), EBV-transformed LCLs (CZE and IHE; **B**), and mutant p53 cells (DG-75 and HL-60; **C**) were treated with 7 μM Nutlin-3a or vehicle control for the indicated time periods. Cells were pulse-labeled with BrdU and analyzed for DNA content by flow cytometry. BrdU incorporation during the S phase is indicated as percentage of stained cells. The sub-G_1 populations in PEL cells are denoted by arrows. Data are representative of 3 independent experiments.

tinguishable from those of untreated controls (Figure 2C). This confirmed that Nutlin-3a induces a G_1 cell-cycle arrest in WT p53 cells, and suggests selective induction of massive cell death only in the KSHV-infected PEL cells.

Nutlin-3a selectively kills KSHV-infected cells, but not EBV-infected cells. Nutlin-3a possesses antiproliferative activity in a variety of cancer cell lines and leukemias (16, 33–36). To investigate the cytotoxic effect of MDM2 inhibition in KSHV lymphomas, we incubated PEL cell lines, EBV-transformed LCLs, and p53 mutant cell lines with Nutlin-3a and determined cell viability by trypan blue exclusion. Nutlin-3a reduced cell viability in KSHV-infected PEL cell lines BC-1, BC-3, and BCBL-1 as well as in KSHV-infected LCL IHH (Figure 3A). After 5 days of treatment, only 2.8% of BC-1, 6.5% of BC-3, and 35% of BCBL-1 cells were viable compared with mock-treated control cells. In contrast, Nutlin-3a had no effect on cell viability of the 2 KSHV-negative EBV-transformed LCLs (CZE, 86%; IHE, 84%; Figure 3A). As expected, there was no effect on the viability of the p53 mutant cells by Nutlin-3a (Figure 3A).

To confirm that the cytotoxic effect of Nutlin-3a in PEL cells was caused by apoptosis, we incubated PEL cells, EBV-transformed LCLs, and p53 mutant cells with Nutlin-3a or vehicle control and collected samples up to 120 hours after incubation. Apoptosis was determined by annexin V binding assay followed by flow cytometry (Figure 3, B and C). Use of annexin V staining in combination with propidium iodide (PI) allows separation of cells at early phases of apoptosis (annexin V–positive, PI-negative) from those at the later stages of cell death (annexin V– and PI-positive). Nutlin-3a induced rapid apoptosis in BC-1 cells: 30% of the cells were at early apoptosis after 24 hours of treatment, compared with 4.3% in the control cells. By 72 hours,

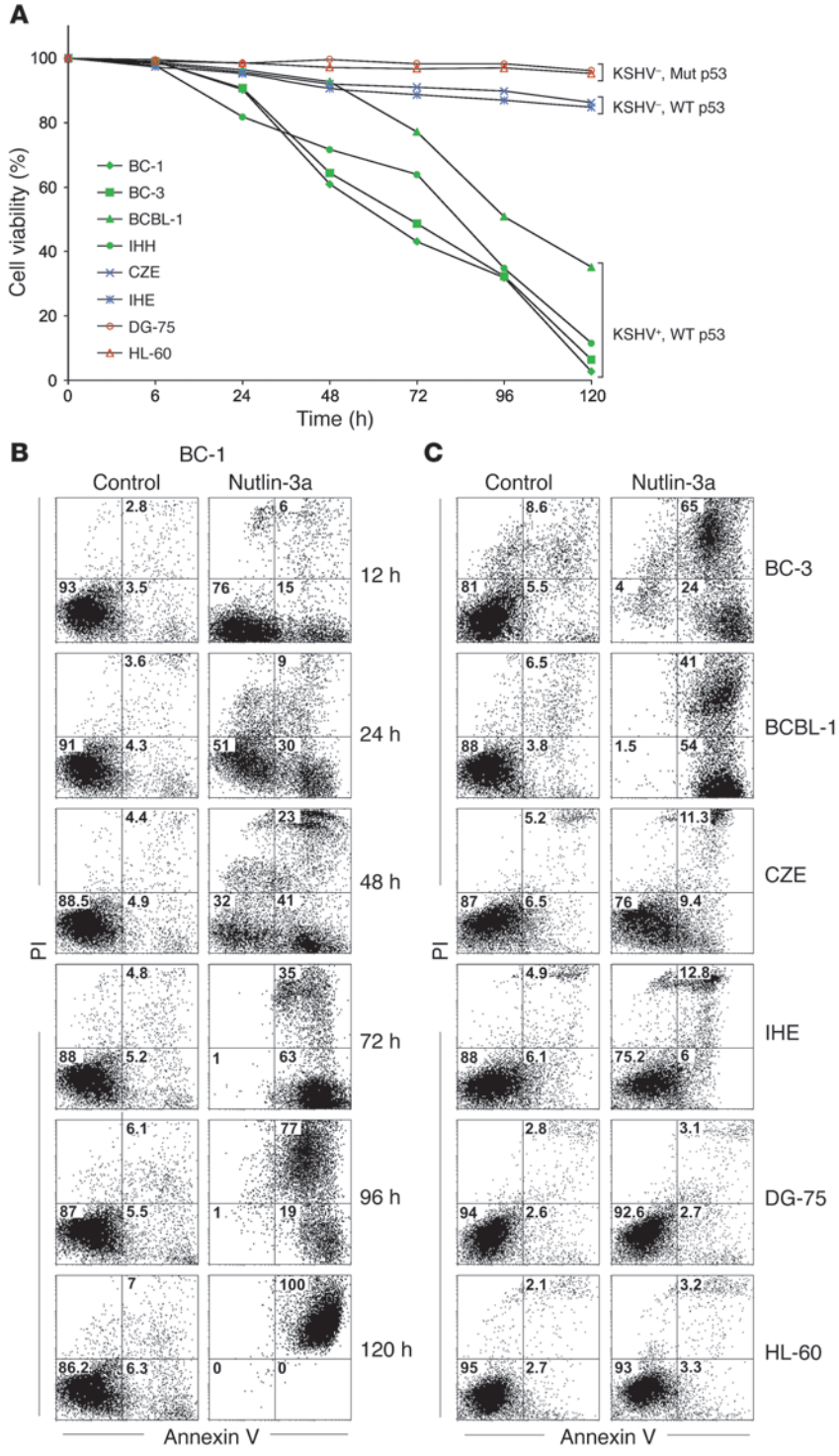

Figure 3
Nutlin-3a has cytotoxic activity in PEL cells. (**A**) PEL cell lines (BC-1, BC-3, and BCBL-1) and KSHV-infected LCL IHH (green symbols), EBV-transformed LCLs (CZE and IHE; blue symbols), or mutant p53 cells (DG-75 and HL-60; red symbols) were cultured for 5 days with 7 μM Nutlin-3a. Cell viability was determined by trypan blue exclusion at the indicated time points. Results are shown as survival curves denoting percentage of viable cells relative to the vehicle control. Data represent the mean of 3 independent experiments. (**B**) Scatter plot of annexin V–FITC/PI flow cytometry of BC-1 cells after exposure to 7 μM of Nutlin-3a or vehicle control for different time periods. (**C**) Apoptosis in BC-3, BCBL-1, CZE, IHE, DG-75, and HL-60 cells was assessed at 96 hours after treatment with 7 μM Nutlin-3a or vehicle control by annexin V–FITC/PI binding and measured by flow cytometry analysis. Lower left quadrants represent viable cells (annexin V– and PI-negative); lower right quadrants represent early apoptotic cells (annexin V–positive, PI-negative) demonstrating cytoplasmic membrane integrity; upper right quadrants represent nonviable, late apoptotic cells (annexin V– and PI-positive). Numbers indicate the percentage of cells in each quadrant. Shown is 1 representative experiment of 3.

63% of the Nutlin-3a–treated BC-1 cell population was at early apoptosis and 35% was at the late stage; thus, 98% of cells were apoptotic at this time point. After 96 and 120 hours, Nutlin-3a treatment dramatically increased the population of late apoptotic cells in the BC-1 line to 77% and 100%, respectively (Figure 3B). A strong apoptotic response was observed in BC-3 and BCBL-1 cells at 96 hours, whereas treatment of the EBV-transformed LCLs or the p53 mutant cell lines did not lead to increased apoptosis (Figure 3C). These results confirmed that Nutlin-3a selectively kills KSHV-associated lymphomas in a p53-dependent manner.

KSHV infection promotes cell killing by Nutlin-3a. We next investigated whether infection of cells by KSHV specifically promotes the cell-death program induced by Nutlin-3a. To this end, we used U2OS osteosarcoma cells and EA.hy 926 endothelial cells (37), both harboring WT p53, which were de novo infected

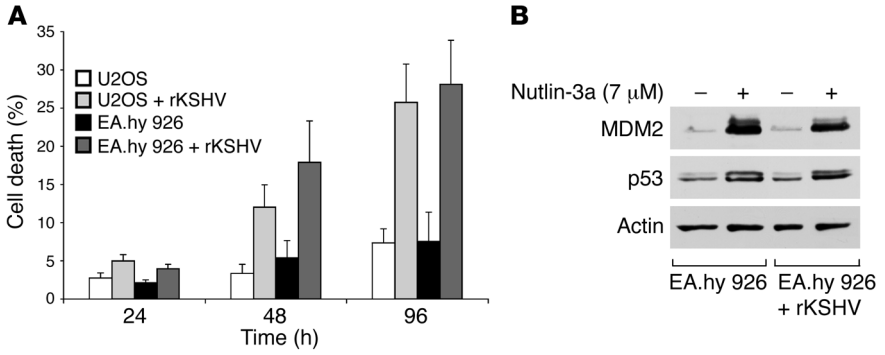

Figure 4

Nutlin-3a selectively kills KSHV-infected cells. (**A**) U2OS and EA.hy 926 cells in the absence or presence of latent rKSHV infection were treated with 7 μM Nutlin-3a, and cell death was assessed by trypan blue exclusion at 24, 48, and 96 hours of treatment. Values represent the percentage of dead cells induced by Nutlin-3a treatment. The percentage of dead cells in the DMSO control was subtracted as a background. Each value represents the mean of 3 independent experiments. (**B**) Noninfected and rKSHV-infected EA.hy 926 cells were incubated for 12 hours in the presence or absence of 7 μM Nutlin-3a. Whole-cell lysates were subjected to SDS-PAGE followed by Western blotting and analyzed for p53 and MDM2 expression. Actin immunoblot is shown as a loading control.

with a recombinant KSHV (rKSHV) (38). rKSHV expresses red fluorescent protein (RFP) from the KSHV lytic PAN promoter and GFP from the cellular EF-1α promoter. All of the rKSHV-infected EA.hy 926 and U2OS cells were positive for GFP, and the establishment of latent infection was confirmed by indirect immunofluorescence using anti-LANA antibodies (data not shown). Less than 1% of the cells expressed RFP, indicating the absence of lytic replication. However, we successfully induced lytic replication by treating the cells with a baculovirus expressing RTA and Na-butyrate (data not shown). These KSHV-infected cells and their parental noninfected cell lines were treated with Nutlin-3a, and its cytotoxic effect was determined by trypan blue exclusion. The percentage of dead cells increased about 4-fold following 96 hours of Nutlin-3a treatment in the KSHV-infected cells compared with uninfected cells (Figure 4A). Western blotting of cell extracts from the noninfected and rKSHV-infected EA.hy 926 cells confirmed accumulation of p53 and MDM2 in response to Nutlin-3a treatment (Figure 4B). Based on these results, we conclude that the MDM2 inhibitor selectively induces cytotoxic activity in KSHV-infected cells.

Activated DNA damage response in KSHV lymphomas enhances cytotoxicity by Nutlin-3a. One plausible mechanism for the conversion of the cytostatic Nutlin-3a response to a cytotoxic response is suggested by a recent report indicating that intrinsic DNA damage signaling in cancer cells is critical in regulating Nutlin-3a–induced apoptosis (27). We therefore investigated whether PEL and KSHV-negative EBV-transformed LCLs show signs of activated DNA damage signaling. To this end, the KSHV-positive BC-1, BC-3, and BCBL-1 cell lines and the EBV-transformed LCLs CZE and IHE were immunostained with an antibody against γH2AX, the phosphorylated form of histone H2AX. Phosphorylation of histone H2AX (detected by γH2AX focal staining) is a commonly used marker of the DNA damage response activated by replication stress and double-stranded DNA breaks (39, 40). Quantitative indirect immunofluorescence analysis revealed sustained γH2AX-positive foci in 72%, 62%, and 54% of BC-1, BC-3, and BCBL-1 cells, respectively, while the EBV-transformed LCLs showed remarkably fewer cells positive for γH2AX focal staining (CZE, 19%; IHE, 21%; Figure 5, A and B). We also analyzed the level of phosphorylation on Chk2 at threonine 68, another marker for activated DNA damage response, in BC-1, BC-3, and BCBL-1 cells as well as the EBV-transformed LCLs and the p53 mutant cell lines. Elevated levels of phosphorylated Chk2(Thr68) were observed in BC-1 and BC-3 cells 12 hours after exposure to Nutlin-3a (Figure 5C).

To obtain additional evidence in support of the role of activated DNA damage response as an effector for Nutlin-3a cytotoxicity, we subjected the EBV-transformed LCLs to gamma irradiation (1 Gy) and compared cell viability after Nutlin-3a treatment with that of nonirradiated cells. Induction of DNA damage by irradiation was confirmed by an increase in γH2AX focal staining (data not shown). After 4 days of treatment, there was a 2.6-fold increase in the cell death of irradiated versus nonirradiated Nutlin-3a–treated IHE cells (Figure 5D). Similar results were obtained with the other EBV-transformed LCL, CZE (data not shown). To further explore the involvement of DNA damage checkpoint activation in Nutlin-3a–induced cytotoxicity, we pretreated the KSHV-infected PEL cell line BC-1 and LCL IHH as well as irradiated and nonirradiated EBV-transformed LCL IHE with an inhibitor of the ATM-Chk2 pathway (caffeine) for 24 hours followed by exposure to Nutlin-3a. Abrogation of the ATM-Chk2 pathway led to a substantial decrease in Nutlin-3a–induced cytotoxicity of KSHV-infected cell lines (BC-1 and IHH) and irradiated IHE cells (Figure 5D). Taken together, these results demonstrate that activation of the DNA damage response in KSHV lymphomas increases the sensitivity of KSHV-positive cells to Nutlin-3a–induced cell death.

Disruption of the p53-MDM2-LANA complex triggers the cytotoxic effect of Nutlin-3a in KSHV lymphomas. Nutlins were designed to inhibit interaction of MDM2 with p53 and to disrupt complex formation between the 2 proteins (15). Consequentially, they stabilize and activate p53 by blocking its MDM2-mediated degradation. To address whether any KSHV-encoded proteins complex with p53 and MDM2, we performed gel filtration chromatography of PEL cells in the absence and presence of Nutlin-3a treatment. In a BC-3 control cell extract, p53 and MDM2 coeluted at 660–440 kDa (Figure 6A). No monomeric p53 was detected in the gel filtration fractions (data not shown), suggesting that most — if not all — p53 is associated with MDM2. To gain more insight into the specificity of the effect of Nutlin-3a in KSHV-infected cells, we addressed the distribution of the KSHV latent protein LANA in BC-3 cell extract prior to and after Nutlin-3a treatment. Previous studies have suggested that LANA associates with p53 and inhibits p53-mediated apoptosis (26). Interestingly, LANA coeluted with the p53-MDM2 complex, indicating a high-order molecular complex among p53, MDM2, and LANA in untreated PEL cells (Figure 6A). Identical profiles were also obtained from BC-1 and BCBL-1 cell extracts (data not shown). Treatment of BC-3 cells with Nutlin-3a for 12

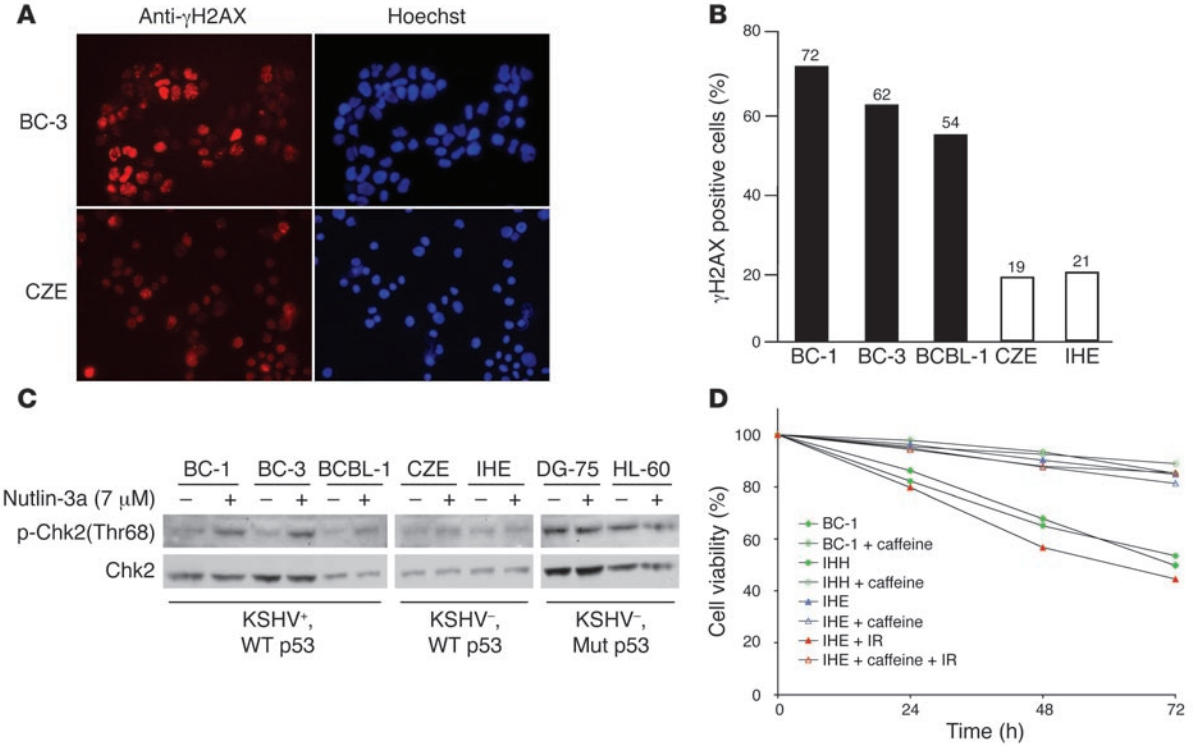

Figure 5

DNA damage signaling enhances the cytotoxic effect of Nutlin 3a. (**A**) BC-3 and CZE cells were immunostained with antibody against γH2AX, the phosphorylated form of histone H2AX. The nuclear morphology was visualized by Hoechst staining. (**B**) Percentage of γH2AX-positive cells in PEL cells (BC-1, BC-3, and BCBL-1) and EBV-transformed LCLs (CZE and IHE). Results represent the mean of 2 independent experiments. (**C**) BC-1, BC-3, BCBL-1, CZE, IHE, DG-75, and HL-60 cells were incubated for 12 hours in the presence or absence of 7 μM Nutlin-3a. Whole-cell lysates were subjected to SDS-PAGE followed by Western blotting and analyzed for phosphorylated Chk2(Thr68) and total Chk2 expression. (**D**) Survival curves for BC-1, IHH, and IHE cells (some gamma-irradiated at 1 Gy; IR) incubated with Nutlin-3a in the presence or absence of caffeine (2 mM). Cell death was determined by trypan blue exclusion at 24, 48, and 72 hours after treatment. Values represent the percentage of viable cells relative to that of DMSO control.

hours resulted in a dramatic redistribution of p53, MDM2, and LANA in the eluted fractions. Importantly, this abrogated the co-elution of MDM2 and LANA with p53, suggesting disruption of interactions among these proteins (Figure 6A).

To analyze the formation of the p53-MDM2-LANA complex in BC-3 cells and to explore the effect of Nutlin-3a on this complex, we performed reciprocal immunoprecipitations for p53 and MDM2. High–molecular weight gel filtration fractions (600–400 kDa) from mock- and Nutlin-3a–treated BC-3 cells were subjected to immunoprecipitation with anti-p53 or anti-MDM2 antibodies. Western blot analysis of the resulting coprecipitates from mock-treated fractions revealed that LANA and MDM2 coprecipitated with p53 antibodies and, conversely, that LANA and p53 coprecipitated with MDM2 (Figure 6B). This demonstrates that p53, MDM2, and LANA associate in vivo in PEL cells. Treatment of BC-3 cells with Nutlin-3a destroyed the interaction of LANA with p53 and markedly decreased the amount of LANA coprecipitating with MDM2 (Figure 6B). As expected, the interaction between p53 and MDM2 was also abolished upon 12 hours' treatment with Nutlin-3a (Figure 6B). Taken together, these results identify LANA as a component of the p53-MDM2 complex and demonstrate that Nutlin-3a disrupted the complex in KSHV lymphoma cells. This may contribute to the specificity and efficiency of Nutlin-3a–mediated cell death in KSHV lymphomas.

Nutlin-3a is a potent agent for treating KSHV lymphomas in vivo. Because in vitro experiments cannot fully mimic all aspects of tumorigenesis and predict potential therapeutic value, we assessed the effect of Nutlin-3a on KSHV lymphomas in vivo. The antitumor activity of Nutlin-3a was evaluated in a BC-3 cell–based xenograft model (41). The most crucial preclinical evaluation of an antitumor agent is to determine its ability to induce responses in established tumors. BC-3 cells were implanted subcutaneously into Balb/c nude female mice and allowed to grow until the tumors were palpable. Administration of 20 mg/kg Nutlin-3a every other day for 2 weeks (7 doses) caused marked regression of all tumors in the treated animals, whereas none of the animals receiving vehicle control showed tumor regression during this time course (Figure 7). Nutlin-3a was well tolerated without any weight loss or other obvious signs of toxicity. All animals (n = 8) treated with Nutlin-3a showed a significant reduction (approximately 40%; P = 0.02) in BC-3 tumor volume at day 10 after starting treatment (Figure 7). Three mice showed complete tumor regression, and follow-up of these mice for over 90 days did not indicate any recurrence of the tumor growth. After cessation of the treatment, tumors with partial responses started to grow again, but the size of these tumors remained radically smaller than in the control mice (223 mm^3 versus 436 mm^3), and they remained susceptible to Nutlin-3a treatment. As expected,

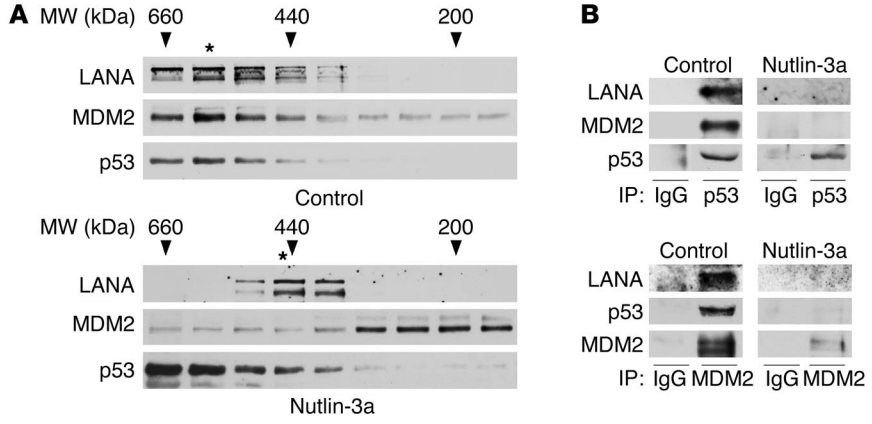

Figure 6
Nutlin-3a disrupts the p53-MDM2-LANA interaction. (**A**) Extracts from the BC-3 cell line exposed for 12 hours to vehicle control or 7 μM Nutlin-3a were separated using gel filtration chromatography. Fractions were analyzed by Western blotting with antibodies against p53, MDM2, and LANA. The elution profile of molecular weight standards is indicated above the lanes. (**B**) The peak fractions for LANA (asterisks in **A**) from BC-3 cells treated with either vehicle control or 7 μM Nutlin-3a for 12 hours were used in immunoprecipitations with anti-p53 or anti-MDM2 antibodies. As a control, a duplicate sample from the same fraction was immunoprecipitated with mouse IgG. Immunocomplexes were resolved by SDS-PAGE and analyzed by Western blotting with antibodies against p53, MDM2, and LANA.

tumors originating from the p53 mutant cell line HL-60 did not respond to the Nutlin-3a treatment described above (data not shown). These results demonstrate that p53 reactivation via Nutlin-3a is an efficient treatment for KSHV-lymphomas in mice and suggest a potential therapeutic strategy for treatment of these fatal virus-induced malignancies in humans.

Discussion

This study provides what we believe to be a novel principle for the efficient treatment of KSHV-induced lymphomas through reactivation of the p53 pathway by a small-molecule inhibitor of the p53-MDM2 interaction, Nutlin-3a. Although *p53* mutations occur rarely in KS or PELs (25), our results demonstrate that inactivation of p53-mediated processes occurred through binding of the viral protein LANA to the p53-MDM2 complex in these lymphomas. Nutlin-3a treatment resulted in disruption of interactions among all 3 proteins in this complex and induced cytotoxicity at concentrations that were nonapoptotic in EBV-transformed LCLs, which express WT p53. In line with our results, p53 target gene induction as well as growth inhibition and apoptosis of PEL cells was recently reported by Petre et al. (42). The specificity of the cytotoxic effect of Nutlin-3a on KSHV-infected cells implies that KSHV infection is a factor converting p53 pathway activation from cytostatic (i.e., p21-induced) to pro-apoptotic. Intriguingly, EBV also encodes proteins suggested to bind p53 or to interfere with its function (43–45), but this did not render the EBV-transformed LCLs sensitive to Nutlin-3a–induced apoptosis.

Another possible explanation for the efficiency of Nutlin-3a killing of KSHV-infected cells could be a recently described property intrinsic to cancer cells: the activation of DNA damage signaling (40, 46). Accordingly, 53BP1, a component of the ATM-Chk2 DNA damage checkpoint pathway (30), was identified as a critical mediator of cellular cytotoxicity by Nutlin-3a (27). In addition, cytotoxic drugs have been shown to synergize with Nutlin-3a in inducing apoptosis of different leukemia and multiple myeloma cell lines (33–36). We detected pronounced activation of DNA damage signaling in all PEL cell lines studied compared with EBV-transformed LCLs by analyzing the levels of phosphorylated Chk2(Thr68) or focal staining of the DNA damage marker γH2AX. Furthermore, the EBV-transformed LCLs could be sensitized to Nutlin-3a–mediated cell killing by subjecting them to a low dose of gamma irradiation. Moreover, by inhibiting DNA damage checkpoint signaling, we protected KSHV lymphoma cells as well as irradiated EBV-transformed LCLs from Nutlin-3a–induced cell killing. The activated DNA damage response may cause increased levels of p53 (and MDM2); however, these were inactivated by the association to LANA. This implies that intrinsic DNA damage signaling, together with the complex formation among p53, MDM2, and LANA in KSHV lymphomas, may contribute to the selectivity and efficiency of Nutlin-3a–induced cell death.

The AIDS epidemic has had a major impact on the prevalence of KSHV, and the vast majority of PELs occur in HIV-seropositive individuals. Currently there is no efficient treatment for PEL, and the treatment modalities in use consist mostly of cytostatic drugs with DNA-damaging activities, which are neither potent nor selective for this malignancy (reviewed in ref. 21). The highly

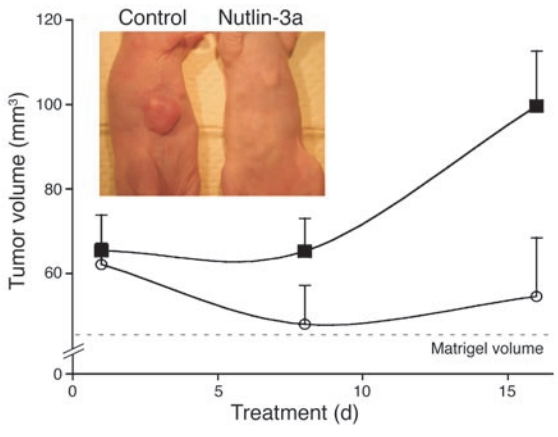

Figure 7
Antitumor activity of Nutlin-3a in vivo. Growth curves of Nutlin-3a– and vehicle control–treated BC-3 tumors. Balb/c nude mice were injected subcutaneously with 6×10^6 BC-3 cells. When the tumors had grown to palpable size, the mice were treated intraperitoneally with the vehicle control (filled squares) or 20 mg/kg of Nutlin-3a (open circles). Nutlin-3a treatment resulted in regression of tumors; at the end of treatment, these tumors were significantly smaller than those treated with vehicle ($P = 0.02$). Dashed line indicates the volume of Matrigel in the tumor. Data (mean and SEM) are representative of 2 independent experiments. Inset shows a photograph of BC-3 tumor–bearing Balb/c nude mice treated with either vehicle control or 20 mg/kg Nutlin-3a 7 times over the course of 2 weeks.

active antiretroviral therapy (HAART) to treat AIDS has also proven effective for treatment of KS and PEL, but its use is restricted to patients with asymptomatic and non–life-threatening PELs (47). Development of specific and efficient therapy for KSHV-related malignancies requires better understanding of the pathways it uses for tumorigenic conversion. Here we demonstrated that the p53 pathway was inactivated in PELs and that selective disruption of the p53-MDM2-LANA complex by Nutlin-3a showed remarkable therapeutic activity in our PEL xenograft model in vivo. Importantly, the MDM2 inhibitor showed no toxic effects in previous studies with oral administration of doses 10 times higher than were used in our study (15, 16). Taken together, our data demonstrate that Nutlin-3a selectively and efficiently kills KSHV lymphoma cells. We therefore believe that reactivation of the p53 apoptotic pathway by Nutlin-3a offers a novel and valuable strategy for treatment of PEL in the future.

Methods

Cell lines. PEL cell line BC-1 is derived from a HIV-positive patient. The cell line is coinfected with KSHV and EBV and was obtained from the ATCC. The BC-3 and BCBL-1 cell lines are negative for HIV and infected only with KSHV (48, 49). BC-3 and BCBL-1 cells were kindly provided by E. Cesarman (Cornell Medical College, New York, New York, USA). EBV-transformed LCLs, CZE and IHE, were established from peripheral blood B cells of healthy donors. DG-75 Burkitt lymphoma and HL-60 human promyelocytic leukemia cell lines were purchased from the ATCC. PEL cell lines and KSHV-negative control cells were cultured in a humidified 5% CO_2 atmosphere at 37°C in RPMI 1640 medium supplemented with 15% FCS (Invitrogen), 100 U/ml penicillin G, and 100 μg/ml streptomycin. U2OS human osteosarcoma (ATCC) and EA.hy 926 endothelial cells (a gift from K. Alitalo, University of Helsinki, Helsinki, Finland) were grown in DMEM supplemented with 10% FCS (Invitrogen), 100 U/ml penicillin G, and 100 μg/ml streptomycin. The EA.hy 926 endothelial cell line is derived by fusing human umbilical vein endothelial cells with the permanent human cell line A549 (37), and it retains WT p53 as well expression of several endothelial cell markers and properties (50).

Establishment of EBV-transformed and KSHV-infected LCLs. PBMCs were isolated from EDTA-treated blood of 2 healthy individuals by discontinuous gradient centrifugation (Lymphoflot; Biotest). To induce the expression of lytic viral proteins in EBV-positive B95-8 or KSHV-positive BCBL-1 cells, cells were treated with either 20 ng/ml phorbol 12-myristate 13-acetate (TPA; Sigma-Aldrich) or 3 mM sodium *n*-butyrate (Sigma-Aldrich) for 24 hours. Supernatants of the B95-8 or BCBL-1 cells grown at densities greater than 5×10^5/ml were filtered through 0.4-μm filters and serially diluted in flat-bottomed 96-well microtiter plates. Subsequently, PBMCs were added at a density of 10^4 cells per well. The culture medium used to generate LCLs contained RPMI, 20% heat-inactivated FCS, 100 IU/ml penicillin, 100 mg/ml streptomycin, 2 mM L-glutamine, 1 mM sodium pyruvate (Invitrogen), 20 mM bathocuproine disulfonic acid, and 50 μm/ml α-thioglycerol (Sigma-Aldrich).

rKSHV.219 production and infection. Vero cells latently infected with a GFP-expressing rKSHV (rKSHV.219), a kind gift from J. Vieira (University of Washington, Seattle, Washington, USA), were used to produce infectious virus as described in Vieira et al. (38). In brief, 80%–90% confluent rKSHV.219 Vero cells in 6-well plates were reactivated by adding 400 μl/well of a recombinant baculovirus (BacK50) expressing the KSHV lytic activator ORF 50 (RTA; a gift from J. Vieira) for 2 hours, removed, and replaced with complete media containing 1.25 mM sodium butyrate (Sigma-Aldrich). Butyrate was removed 24 hours after reactivation, and supernatants containing rKSHV.219 were collected 48 hours later. U2OS and EA.hy 926 cells were plated at a density of 2×10^5 cells per well in a 6-well dish and were infected the next day with 1.0 ml/well of rKSHV.219 virus supernatant in the presence of 8 μg/ml polybrene to enhance their infectivity. The plates were spin-transduced by centrifugation at 1,050 *g* (Heraeus Multifuge 3S-R; SeqLab) for 30 minutes at room temperature. Cells were returned to 37°C at 5% CO_2 for 1.5 hours, after which the rKSHV.219 supernatant was replaced with complete media. Cells were routinely cultured in a humidified 5% CO_2 atmosphere at 37°C in DMEM containing 10% (w/v) FCS, 100 U/ml penicillin, and 100 μg/ml streptomycin in the presence of 1 μg/ml puromycin, which was included 2 days after infection.

Protein analysis and immunofluorescence. Western blotting analysis, immunoprecipitations, and gel filtration chromatography were carried out as described previously (51). Gel filtration chromatography was performed on a Superdex 200 HR column (Amersham Pharmacia). The following primary antibodies were used: anti-p53 (DO-1 and FL-393), anti-MDM2 (SMP-14 and 2A10), anti-actin (C-2), and anti-Bax (B-9; Santa Cruz Biotechnology Inc.); anti-MDM2 (IF-2; Oncogene Sciences); anti-LANA (HHV8-ORF73; ABI Biotechnologies); anti-p21 (SX118; BD Biosciences — Pharmingen); anti-53BP1 (Novus Biologicals); anti–phosphorylated p53(Ser15), anti–phosphorylated Chk2(Thr68), and anti-Chk2 (DCS-270; Cell Signaling Technology). A mixture of the 3 indicated monoclonal antibodies against MDM2 was used for its detection. HRP-conjugated antibodies specific for rabbit, mouse, or rat immunoglobulins were purchased from Chemicon International. Cytocentrifugation and indirect immunofluorescence were performed as previously described (51). PEL cell lines and EBV-transformed LCLs were labeled with a mouse monoclonal antibody against γH2AX (Upstate USA Inc.) and Alexa Fluor 594–conjugated antibody to rabbit immunoglobulin (Invitrogen). The fluorochromes were visualized with a Zeiss Axioplan 2 fluorescent microscope equipped with Zeiss PLAN-NEOFLUOR ×40/0.50 numeric aperture objective lens. Images were acquired with a Zeiss Axiocam HRc, using Zeiss AxioVision (version 4.5 SP1) and Adobe Photoshop software (version 7.0; Adobe).

Drug treatment and viability determination. PEL cells, EBV-transformed LCLs, KSHV-infected LCLs, and p53 mutant cells suspended at 2×10^5 cells/ml were incubated with 7 μM Nutlin-3a (Alexis Biochemicals) or relative amount of the solvent (vehicle; 0.1% DMSO) for the indicated time. rKSHV-infected and noninfected parental U2OS and EA.hy 926 cells were plated at a density of 0.5×10^5 cells per well in 24-well plates, and after 48 hours the cells were treated with 7 μM Nutlin-3a. Cell viability was determined by trypan blue exclusion (Sigma-Aldrich). The control treatment with DMSO was always included, and the relative survival in each assay was calculated as the percentage of live cells relative to the live cell population in the control. Results are from 2–3 independent experiments. To inhibit the ATM-Chk2 pathway in KSHV-infected PEL cell line BC-1, KSHV-infected LCL IHH, or EBV-transformed LCL IHE, the cells were pretreated with 2 mM caffeine (Sigma-Aldrich) for 24 hours before the Nutlin-3a treatment. Caffeine was kept constant during the exposure to Nutlin-3a.

Measurement of cell proliferation and apoptosis. The proportion of cells at the S phase was determined by measuring incorporation of BrdU and PI into the DNA. Cells were grown at a density of 2×10^5 cells/ml 24 hours prior to the treatment with Nutlin-3a. The cells were pulse-labeled with 25 μM BrdU (Sigma-Aldrich) for 30 minutes and fixed in ice-cold 70% ethanol. After fixation, the cells were washed in PBS and treated with 3.5 N HCl for 30 minutes at room temperature. After washing in a neutralizing washing buffer (0.1% BSA/PBS), the cells were incubated with an anti-BrdU antibody (Dako) for 45 minutes. Alexa Fluor 488–conjugated (Invitrogen) secondary antibody was used for detection. Finally, the cells were stained with 30 μg/ml PI (Invitrogen) in PBS supplemented with 50 μg/ml RNase (Sigma-Aldrich) for 30 minutes at 37°C. Apoptosis was measured by dual-labeling with the Annexin V–FITC Apoptosis Detection kit I (BD Biosciences —

Pharmingen) according to the manufacturer's instructions and analyzed by flow cytometry. Labeled cells were acquired using a BD-LSR Flow Cytometer (BD Biosciences), and the cell populations were analyzed by CellQuest software (version 3.3; BD).

Human tumor xenografts. Female Balb/c nude mice (4–6 weeks old) were obtained from Taconic Europe and maintained under specific pathogen–free conditions in a temperature- and humidity-controlled environment. Mice under anesthesia were injected subcutaneously with 6×10^6 BC-3 or HL-60 cells in 50% Matrigel (BD Biosciences). Treatment was started intraperitoneally after the tumors were established (i.e., palpable). Nutlin-3a (20 mg/kg) or the vehicle control was administered every second day for a total of 2 weeks (7 doses). Tumor volumes were measured with a caliper and calculated according to the formula V = width × height × depth/2, derived from the formula for the volume of an ellipsoid (52). In order to monitor the health of the animals, the mice were weighed once per week. All animal studies were conducted in accordance with the guidelines of the Provincial Government of Southern Finland, and the protocol was approved by the Experimental Animal Committee of the University of Helsinki.

Statistics. Statistical analyses were performed using ANOVA. P values less than 0.05 were considered significant.

Acknowledgments

We thank T.P. Mäkelä, A. Lehtonen, and A. Järviluoma for discussions, suggestions, and critical review of this manuscript; J. Vieira and K. Alitalo for providing reagents; S. Koopal and C. Pussinen for providing rKSHV-infected EA.hy 926 cells; and J. Furuhjelm for preparing the rKSHV-infected U2OS cells. We also thank K. Peltonen for help with flow cytometry. J. Barlund is acknowledged for excellent technical assistance. This work was supported by grants from the Academy of Finland (P.M. Ojala and P. Laakkonen), the Centre of Excellence in Translational Genome-Scale Biology (P.M. Ojala), and the Centre of Excellence in Cancer Biology (M. Laiho), and additional funds were provided by the Academy of Finland Research Program for Systems Biology and Bioinformatics (P.M. Ojala), the Finnish Cancer Foundation (P.M. Ojala and M. Laiho), the Sigrid Juselius Foundation (P.M. Ojala, P. Laakkonen), and the European Union (FP6 INCA project LSHC-CT-2005-018704 to P.M. Ojala). G. Sarek and S. Kurki have been supported by the University of Helsinki Graduate School in Biotechnology and Molecular Biology.

Received for publication November 13, 2006, and accepted in revised form January 23, 2007.

Address correspondence to: Päivi M. Ojala, Genome-Scale Biology Program, Institute of Biomedicine, Biomedicum Helsinki, PO Box 63 (Haartmaninkatu 8), FIN-00014 University of Helsinki, Helsinki, Finland. Phone: 358-9-191-25548; Fax: 358-9-191-25554; E-mail: Paivi.Ojala@helsinki.fi.

Sari Kurki and Juulia Enbäck contributed equally to this work.

1. Chang, Y., et al. 1994. Identification of herpesvirus-like DNA sequences in AIDS-associated Kaposi's sarcoma. *Science.* **266**:1865–1869.
2. Soulier, J., et al. 1995. Kaposi's sarcoma-associated herpesvirus-like DNA sequences in multicentric Castleman's disease. *Blood.* **86**:1276–1280.
3. Cesarman, E., et al. 1995. In vitro establishment and characterization of two acquired immunodeficiency syndrome-related lymphoma cell lines (BC-1 and BC-2) containing Kaposi's sarcoma-associated herpesvirus-like (KSHV) DNA sequences. *Blood.* **86**:2708–2714.
4. Ablashi, D.V., Chatlynne, L.G., Whitman, J.E., Jr., and Cesarman, E. 2002. Spectrum of Kaposi's sarcoma-associated herpesvirus, or human herpesvirus 8, diseases. *Clin. Microbiol. Rev.* **15**:439–464.
5. Cesarman, E., and Knowles, D.M. 1999. The role of Kaposi's sarcoma-associated herpesvirus (KSHV/HHV-8) in lymphoproliferative diseases. *Semin. Cancer Biol.* **9**:165–174.
6. Carbone, A., and Gloghini, A. 2005. AIDS-related lymphomas: from pathogenesis to pathology. *Br. J. Haematol.* **130**:662–670.
7. Jarviluoma, A., and Ojala, P.M. 2006. Cell signaling pathways engaged by KSHV. *Biochim. Biophys. Acta.* **1766**:140–158.
8. Vogelstein, B., Lane, D., and Levine, A.J. 2000. Surfing the p53 network. *Nature.* **408**:307–310.
9. Harris, S.L., and Levine, A.J. 2005. The p53 pathway: positive and negative feedback loops. *Oncogene.* **24**:2899–2908.
10. Hollstein, M., Sidransky, D., Vogelstein, B., and Harris, C.C. 1991. p53 mutations in human cancers. *Science.* **253**:49–53.
11. Hermeking, H., and Eick, D. 1994. Mediation of c-Myc-induced apoptosis by p53. *Science.* **265**:2091–2093.
12. Attardi, L.D., Lowe, S.W., Brugarolas, J., and Jacks, T. 1996. Transcriptional activation by p53, but not induction of the p21 gene, is essential for oncogene-mediated apoptosis. *EMBO J.* **15**:3693–3701.
13. Schmitt, C.A., et al. 2002. Dissecting p53 tumor suppressor functions in vivo. *Cancer Cell.* **1**:289–298.
14. Honda, R., Tanaka, H., and Yasuda, H. 1997. Oncoprotein MDM2 is a ubiquitin ligase E3 for tumor suppressor p53. *FEBS Lett.* **420**:25–27.
15. Vassilev, L.T., et al. 2004. In vivo activation of the p53 pathway by small-molecule antagonists of MDM2. *Science.* **303**:844–848.
16. Tovar, C., et al. 2006. Small-molecule MDM2 antagonists reveal aberrant p53 signaling in cancer: implications for therapy. *Proc. Natl. Acad. Sci. U. S. A.* **103**:1888–1893.
17. Boulanger, E., et al. 2005. Prognostic factors and outcome of human herpesvirus 8-associated primary effusion lymphoma in patients with AIDS. *J. Clin. Oncol.* **23**:4372–4380.
18. Keller, S.A., et al. 2006. NF-kappaB is essential for the progression of KSHV- and EBV-infected lymphomas in vivo. *Blood.* **107**:3295–3302.
19. Ghosh, S.K., et al. 2003. Potentiation of TRAIL-induced apoptosis in primary effusion lymphoma through azidothymidine-mediated inhibition of NF-kappa B. *Blood.* **101**:2321–2327.
20. Godfrey, A., Anderson, J., Papanastasiou, A., Takeuchi, Y., and Boshoff, C. 2005. Inhibiting primary effusion lymphoma by lentiviral vectors encoding short hairpin RNA. *Blood.* **105**:2510–2518.
21. Aoki, Y., and Tosato, G. 2004. Therapeutic options for human herpesvirus-8/Kaposi's sarcoma-associated herpesvirus-related disorders. *Expert Rev. Anti Infect. Ther.* **2**:213–225.
22. Simonelli, C., et al. 2003. Clinical features and outcome of primary effusion lymphoma in HIV-infected patients: a single-institution study. *J. Clin. Oncol.* **21**:3948–3954.
23. Nador, R.G., et al. 1996. Primary effusion lymphoma: a distinct clinicopathologic entity associated with the Kaposi's sarcoma-associated herpes virus. *Blood.* **88**:645–656.
24. Carbone, A., et al. 1998. Establishment and characterization of EBV-positive and EBV-negative primary effusion lymphoma cell lines harbouring human herpesvirus type-8. *Br. J. Haematol.* **102**:1081–1089.
25. Katano, H., Sato, Y., and Sata, T. 2001. Expression of p53 and human herpesvirus-8 (HHV-8)-encoded latency-associated nuclear antigen with inhibition of apoptosis in HHV-8-associated malignancies. *Cancer.* **92**:3076–3084.
26. Friborg, J., Jr., Kong, W., Hottiger, M.O., and Nabel, G.J. 1999. p53 inhibition by the LANA protein of KSHV protects against cell death. *Nature.* **402**:889–894.
27. Brummelkamp, T.R., et al. 2006. An shRNA barcode screen provides insight into cancer cell vulnerability to MDM2 inhibitors. *Nat. Chem. Biol.* **2**:202–206.
28. Cai, Q.L., Knight, J.S., Verma, S.C., Zald, P., and Robertson, E.S. 2006. EC5S ubiquitin complex is recruited by KSHV latent antigen LANA for degradation of the VHL and p53 tumor suppressors. *PLoS Pathog.* **2**:e116.
29. Sin, S.H., et al. 2006. Rapamycin is efficacious against primary effusion lymphoma (PEL) cell lines in vivo by inhibiting autocrine signaling. *Blood.* **109**:2165–2173.
30. Wang, B., Matsuoka, S., Carpenter, P.B., and Elledge, S.J. 2002. 53BP1, a mediator of the DNA damage checkpoint. *Science.* **298**:1435–1438.
31. Abraham, R.T. 2002. Checkpoint signalling: focusing on 53BP1. *Nat. Cell Biol.* **4**:E277–E279.
32. Waldman, T., Kinzler, K.W., and Vogelstein, B. 1995. p21 is necessary for the p53-mediated G1 arrest in human cancer cells. *Cancer Res.* **55**:5187–5190.
33. Kojima, K., et al. 2005. MDM2 antagonists induce p53-dependent apoptosis in AML: implications for leukemia therapy. *Blood.* **106**:3150–3159.
34. Stuhmer, T., et al. 2005. Nongenotoxic activation of the p53 pathway as a therapeutic strategy for multiple myeloma. *Blood.* **106**:3609–3617.
35. Coll-Mulet, L., et al. 2006. MDM2 antagonists activate p53 and synergize with genotoxic drugs in B-cell chronic lymphocytic leukemia cells. *Blood.* **107**:4109–4114.
36. Secchiero, P., et al. 2006. Functional integrity of the p53-mediated apoptotic pathway induced by the nongenotoxic agent nutlin-3 in B-cell chronic lymphocytic leukemia (B-CLL). *Blood.* **107**:4122–4129.
37. Edgell, C.J., McDonald, C.C., and Graham, J.B. 1983. Permanent cell line expressing human factor VIII-related antigen established by hybridization. *Proc. Natl. Acad. Sci. U. S. A.* **80**:3734–3737.

38. Vieira, J., and O'Hearn, P.M. 2004. Use of the red fluorescent protein as a marker of Kaposi's sarcoma-associated herpesvirus lytic gene expression. *Virology.* **325**:225–240.
39. DiTullio, R.A., Jr., et al. 2002. 53BP1 functions in an ATM-dependent checkpoint pathway that is constitutively activated in human cancer. *Nat. Cell Biol.* **4**:998–1002.
40. Gorgoulis, V.G., et al. 2005. Activation of the DNA damage checkpoint and genomic instability in human precancerous lesions. *Nature.* **434**:907–913.
41. Staudt, M.R., et al. 2004. The tumor microenvironment controls primary effusion lymphoma growth in vivo. *Cancer Res.* **64**:4790–4799.
42. Petre, C.E., Sin, S.H., and Dittmer, D.P. 2007. Functional p53 signaling in Kaposi's sarcoma-associated herpesvirus (KSHV) lymphomas-implications for therapy. *J. Virol.* **81**:1912–1922.
43. Inman, G.J., and Farrell, P.J. 1995. Epstein-Barr virus EBNA-LP and transcription regulation properties of pRB, p107 and p53 in transfection assays. *J. Gen. Virol.* **76**:2141–2149.
44. Pokrovskaja, K., Mattsson, K., Kashuba, E., Klein, G., and Szekely, L. 2001. Proteasome inhibitor induces nucleolar translocation of Epstein-Barr virus-encoded EBNA-5. *J. Gen. Virol.* **82**:345–358.
45. Kashuba, E., et al. 2003. EBV-encoded EBNA-5 associates with P14ARF in extranucleolar inclusions and prolongs the survival of P14ARF-expressing cells. *Int. J. Cancer.* **105**:644–653.
46. Bartkova, J., et al. 2005. DNA damage response as a candidate anti-cancer barrier in early human tumorigenesis. *Nature.* **434**:864–870.
47. Boulanger, E., Daniel, M.T., Agbalika, F., and Oksenhendler, E. 2003. Combined chemotherapy including high-dose methotrexate in KSHV/HHV8-associated primary effusion lymphoma. *Am. J. Hematol.* **73**:143–148.
48. Arvanitakis, L., et al. 1996. Establishment and characterization of a primary effusion (body cavity-based) lymphoma cell line (BC-3) harboring kaposi's sarcoma-associated herpesvirus (KSHV/HHV-8) in the absence of Epstein-Barr virus. *Blood.* **88**:2648–2654.
49. Renne, R., et al. 1996. Lytic growth of Kaposi's sarcoma-associated herpesvirus (human herpesvirus 8) in culture. *Nat. Med.* **2**:342–346.
50. Rieber, A.J., Marr, H.S., Comer, M.B., and Edgell, C.J. 1993. Extent of differentiated gene expression in the human endothelium-derived EA.hy926 cell line. *Thromb. Haemost.* **69**:476–480.
51. Sarek, G., Jarviluoma, A., and Ojala, P.M. 2006. KSHV viral cyclin inactivates p27KIP1 through Ser10 and Thr187 phosphorylation in proliferating primary effusion lymphomas. *Blood.* **107**:725–732.
52. Schueneman, A.J., et al. 2003. SU11248 maintenance therapy prevents tumor regrowth after fractionated irradiation of murine tumor models. *Cancer Res.* **63**:4009–4016.